

Publication VI

Juha T. Toivanen, Tommi A. Laitinen, Veli-Matti Kolmonen, and Pertti Vainikainen. Reproduction of arbitrary multipath environments in laboratory conditions. IEEE Transactions on Instrumentation and Measurement, accepted for publication.

© 2010 Institute of Electrical and Electronics Engineers (IEEE)

Preprinted, with permission, from IEEE.

This material is posted here with permission of the IEEE. Such permission of the IEEE does not in any way imply IEEE endorsement of any of Aalto University's products or services. Internal or personal use of this material is permitted. However, permission to reprint/republish this material for advertising or promotional purposes or for creating new collective works for resale or redistribution must be obtained from the IEEE by writing to pubs-permissions@ieee.org.

By choosing to view this document, you agree to all provisions of the copyright laws protecting it.

Reproduction of Arbitrary Multipath Environments in Laboratory Conditions

Juha T. Toivanen, Tommi A. Laitinen, Veli-Matti Kolmonen, and Pertti Vainikainen, *Member, IEEE*

Abstract— We discuss the synthesis of arbitrary multipath environments in a spherical volume of space (test zone), with a limited number of feed antennas (probes). The probes can be of any type, e.g., simple dipoles. The required number of probes is proportional to the area of the sphere enclosing the test zone. The signal received by a two-port mobile terminal antenna model placed in the test zone is examined through simulations, using measured real-world propagation channel data. We study how the received signal and the channel capacity are affected by truncation errors and a certain noise level in the probe excitations. This kind of synthesis enables the testing of mobile terminals under realistic operating conditions in laboratory environments. The synthesis is not limited to far-field scenarios, but near-field effects can be generated, as well.

Index Terms—Multipath environment, radio channel, synthesis, MIMO, OTA testing.

I. INTRODUCTION

THE radio channel environment is a crucial factor in determining the link performance of a mobile terminal. It varies significantly according to different signal propagation scenarios, such as urban, rural or indoor. For example, in urban surroundings the number of multipath components arriving from different angles to the mobile terminal is usually high compared to rural environments due to signal reflections from the buildings. Moreover, the radio channel environment seen by a mobile terminal is dynamic, not only because the surroundings are changing, but also because the mobile terminal might be moving. This movement along with the multipath components results in signal fading, which is an important detrimental phenomenon in wireless communication links.

In the product development of mobile terminals, it is naturally of interest to test the mobile terminal performance in realistic operating environments [1], [2]. The advent of MIMO (Multiple-Input Multiple-Output) systems, which exploit the

potential for capacity increase provided by multiple signal propagation paths, makes this kind of testing all the more important. The problem is that field testing of mobile terminals is very time-consuming and expensive, requiring mobile test platforms and field personnel that perform the measurements.

To overcome this problem, various techniques have been proposed. One approach is to use measured radio channel data together with the radiation pattern of the mobile terminal antenna to computationally determine the response of the antenna under the measured conditions [3]. Another method is to try to create an electromagnetic environment with statistical properties similar to those of a certain propagation environment [4].

More accurate reproduction of a multipath environment can be achieved with the use of multiple probes surrounding the device under test (DUT) [5]–[7]. By individually controlling the signals radiated by each probe, e.g., by using a fading emulator, more control over the radio channel parameters is obtained [7]. However, although a related problem has been studied in acoustics [8] [9], the problem of creating truly arbitrary three-dimensional radio channel environments with a limited number of probes has not been addressed. This is an important question because currently there is a lot of interest in the development and standardization of over-the-air (OTA) test methods for MIMO systems [1].

In this paper, we discuss the synthesis of electromagnetic field environments from a spherical wave theory point of view. This approach has several benefits. First, in the general case, the spherical wave theory provides the most efficient representation of electromagnetic fields, requiring a minimum number of terms in the expansion considering the radius of the spherical region of interest. This is important in the synthesis because it translates to a minimum requirement for the number of probes with a test zone of a given size. Second, plane waves of arbitrary direction of arrival and polarization can be synthesized in the test zone, even with a small number of probes. It does not matter what the exact locations of the probes are, but uniform distribution over spherical surface is preferred. Third, since the spherical waves are a complete solution to Maxwell's equations, both near-field and far-field effects can be generated in the same way. This is beneficial because also the near-field effects can be important in some applications (e.g. electromagnetic compatibility testing).

We do not address the question of RF electronics required

Manuscript received November 12, 2009. This work has been funded by the Academy of Finland. Financial support has also been provided by NordForsk, by The Finnish Foundation for Economic and Technology Sciences, by HPY Research Foundation, by The Finnish Society of Electronics Engineers, and by Walter Ahlström's Foundation.

J. T. Toivanen, T. A. Laitinen, V.-M. Kolmonen and P. Vainikainen are with the Aalto University School of Science and Technology, Department of Radio Science and Engineering, SMARAD, P.O. Box 13000, FI-00076 Aalto, Finland, phone: 358-9-4512252, fax: 358-9-4512152, e-mail: juha.toivanen@tkk.fi.

for the synthesis, but instead concentrate on the relevant aspects of the associated electromagnetic theory, assuming harmonic time dependence. We note, however, that such instrumentation exists that can produce appropriate signals with radio channel effects over time and frequency [10].

We study through simulations the effect of truncation errors and noise in the synthesis, using the received signal strength and the channel capacity as the figures of merit. We show that an accurate reproduction of measured (or statistical) propagation environments is possible with a relatively small number of probes and present relations between the accuracy of the test parameters and the number of probes. These relations have been studied in detail earlier in connection with traditional antenna measurements and measurement parameters, but not for MIMO OTA test parameters such as channel capacity [11]. The optimal number of the probes is determined by the required test zone size and by the desired accuracy. The results also show that increasing the number of probes beyond a certain point results in no improvements and is, therefore, useless.

Synthesis of propagation environments in laboratory conditions enables the field tests of mobile terminals to be carried out in the laboratory. This makes the testing easier and allows significant time and cost savings compared to traditional field tests. Moreover, the test scenario is repeatable, which makes it possible to test different designs under identical conditions, thus enabling a fair comparison of their performance.

II. THEORETICAL BACKGROUND

Let us consider a spherical, source-free region of space. Assuming a time dependence of $e^{j\omega t}$, an arbitrary electric field distribution in this region can be expressed in terms of the spherical basis functions as [12]

$$\bar{E}(r, \theta, \varphi) = \frac{k}{\sqrt{\eta}} \sum_{s=1}^{\infty} \sum_{m=-n}^n \sum_{n=-\infty}^{\infty} Q_{smn}^{(1)} \bar{F}_{smn}^{(1)}(r, \theta, \varphi), \quad (1)$$

where \bar{E} is the vectorial electric field; $\bar{F}_{smn}^{(1)}$ are the spherical vector wave functions, with the superscript 1 indicating that both incoming and outgoing waves are present; $Q_{smn}^{(1)}$ are the coefficients of the spherical waves; s , m , and n are the spherical mode indices; r , θ , and φ determine the location in spherical coordinates; k is the wave number; and η is the wave admittance. In the general case, this expansion has an infinite number of terms (index n goes from 1 to infinity). However, when the spherical region is limited in size, the expansion can be appropriately truncated. This can be done because the radial dependence of the spherical Bessel functions is such that higher spherical modes tend rapidly to zero near the origin. The number of effective terms in the expansion then determines the ‘‘dimensionality’’ of the field distribution.

A. Dimensionality of Multipath Fields

It has been shown that both fixed and random multipath

fields in a limited, source-free region of space exhibit an effective finite dimensionality [13], [14]. In other words, there are intrinsic limits in the degrees of freedom of such fields. This makes it possible to truncate the expansion (1) so that n goes from 1 to N , without causing large errors in the result.

In [14] normalized error bounds are derived for a multipath field representation as a function of the truncation number N . It is shown that in a spherical region, the required number of terms in the expansion is proportional to the area of the sphere. This principle is known also from antenna measurement theory [12]. A simple relation that can be used to estimate the required truncation number N based on the radius of the sphere (r_0) is

$$N \approx \lceil kr_0 \rceil, \quad (2)$$

where $\lceil \cdot \rceil$ is the integer ceiling operator. The number of terms J in (1) is

$$J = 2N(N + 2). \quad (3)$$

We can then ask the question how to create the J spherical modes in a laboratory environment with a limited number of probes.

B. Spherical Mode Synthesis

In this section, we will present and discuss two different techniques to synthesize the desired spherical modes in the test zone. Either way, it is necessary to determine the spherical modes produced by the probes in the test zone coordinate system.

The first technique is based on a free-space assumption (i.e., the signal reflections in the measurement chamber are assumed negligible). Furthermore, it requires knowledge of the probe locations and radiation characteristics. The second technique is based on the measurement of the test zone fields produced by the probes and incorporates the effect of signal reflections in the measurement chamber.

1) Technique based on free-space assumption

Assume P probes are placed on a spherical surface, radiating towards the test zone. An example of such a configuration is shown in Fig. 1. In the general case, it is not necessary for the probes to be identical. The radiation characteristics of the probes must be known, and are given by the spherical transmission coefficients $T_{\sigma\mu\nu}^p$. Here, the indices σ , μ , and ν are used for the spherical modes instead of s , m , and n to distinguish the probe coordinate system from the test zone coordinate system, and $p = \{1 \dots P\}$ denotes the probe.

In the test zone coordinate system, the origin is placed in the center of the test zone. The location of each probe in this fixed coordinate system is given by the Euler angles (φ , θ , χ) and the distance from the origin (r). The possible effect of the probe near field in the test zone need not be considered separately, because it is included in the $T_{\sigma\mu\nu}^p$.

With a series of coordinate system rotations and translations, the radiated signal of a probe located at $(r, \varphi, \theta, \chi)$ can be expressed in the test zone coordinate system as [12]

$$\bar{E}_p = \frac{k}{\sqrt{\eta}} \sum_{\sigma\mu\nu} v_p T_{\sigma\mu\nu}^p C_{s\mu n}^{\sigma\nu(3)}(-kr) e^{-i\mu\chi} d_{m\mu}^n(-\theta) e^{-im\varphi} F_{smn}^{(1)}, \quad (4)$$

where v_p is the probe input signal; $C_{s\mu n}^{\sigma\nu(3)}$ are the spherical-wave translation coefficients with the superscript index 3 signifying that translation distance is larger than the probe minimum sphere [12]; and $d_{m\mu}^n$ are the spherical-wave rotation coefficients [12]. Defining the probe coefficients as (note that this is different from the definition in [12]!)

$$P_{smn}^p = \sum_{\sigma\mu\nu} T_{\sigma\mu\nu}^p C_{s\mu n}^{\sigma\nu(3)}(-kr) e^{-i\mu\chi} d_{m\mu}^n(-\theta) e^{-im\varphi} \quad (5)$$

expansion (4) can be written as

$$\bar{E}_p = \frac{k}{\sqrt{\eta}} \sum_{smn} v_p P_{smn}^p F_{smn}^{(1)} \quad (6)$$

Each probe coefficient, therefore, determines how probe p , located at $(r, \varphi, \theta, \chi)$ contributes to the corresponding spherical mode $\bar{F}_{smn}^{(1)}$ in the test zone coordinate system. With a large number of probes, the relative probe weights v_p can be adjusted to produce a desired field in the test zone.

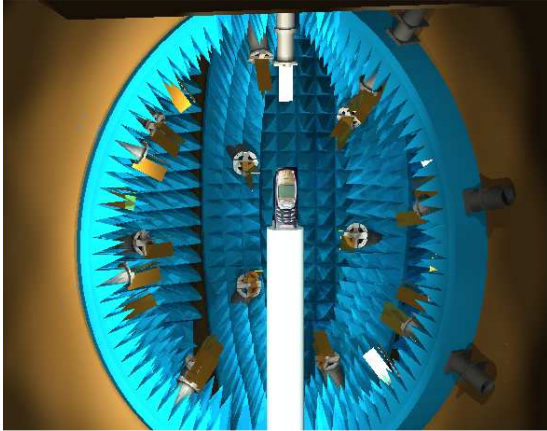


Fig. 1. Illustration of a probe configuration for radio channel environment synthesis. The device under test is placed in the middle in the center of the test zone.

Based on the discussion in the previous section, any multipath field in a limited volume can be expressed with an appropriately truncated expansion. Let this expansion be

$$\bar{E}(r, \theta, \varphi) = \frac{k}{\sqrt{\eta}} \sum_{j=1}^J Q_j^{(1)} \bar{F}_j^{(1)}(r, \theta, \varphi), \quad (7)$$

where the single-index (j) convention has been adopted to replace the spherical mode indices s, m , and n in order to simplify the following expressions [12]. Our goal is now to match the test zone field produced by the probes to (7). We obtain the following matrix equation.

$$\begin{bmatrix} P_1^1 & P_1^2 & \dots & P_1^p \\ P_2^1 & P_2^2 & \dots & P_2^p \\ \vdots & \vdots & \vdots & \vdots \\ P_J^1 & P_J^2 & \dots & P_J^p \end{bmatrix} \begin{bmatrix} v_1 \\ v_2 \\ \vdots \\ v_p \end{bmatrix} = \begin{bmatrix} Q_1 \\ \vdots \\ Q_J \end{bmatrix}, \quad (8)$$

i.e., $\mathbf{P}\mathbf{v} = \mathbf{q}$. Here, matrix \mathbf{P} contains the probe coefficients, determined by the probe radiation characteristics and probe locations. The rows of the matrix correspond to different spherical modes whereas the columns correspond to different probes. Vector \mathbf{v} contains the probe excitations and vector \mathbf{q} the spherical-mode coefficients of the desired test zone field. The required probe excitations can be solved by the Moore-Penrose pseudoinverse [15]

$$\mathbf{v} = \mathbf{P}^\dagger \mathbf{q} = (\mathbf{P}^H \mathbf{P})^{-1} \mathbf{P}^H \mathbf{q}. \quad (9)$$

The conditioning of the problem depends on the \mathbf{P} matrix, which is constant, once the probe locations and characteristics have been fixed. The problem can thus be made well-conditioned by a proper selection of the probe configuration. A uniform configuration over a sphere is likely to produce good results. For exact reproduction of the modes, the number of probes must be larger than or equal to the number of modes. The relation between the number of excitations and the number of modes is discussed in more detail in [9].

This technique does not incorporate the effect of signal reflections in the measurement chamber, because only the direct probe signals are considered in calculating the test zone fields. The reflections may be a significant error source, especially if the number of probes in the chamber is large since the probes also act as reflectors.

2) Technique based on test zone field measurement

It is possible to include the effect of the signal reflections in the synthesis. For this, we must perform a calibration measurement, namely the test zone field (TZF) measurement. The TZF measurement requires an additional, known calibration antenna (the TZF probe), which is rotated in the test zone in order to determine the fields entering the test zone. This technique has the additional advantage that no prior knowledge of the probe characteristics or locations is required.

The TZF measurement has been discussed in detail elsewhere [16] and will not be repeated here. However, the idea is that the spherical-wave coefficients of the TZF

produced by each probe are determined through measurement instead of calculation. We shall denote these coefficients as Z_j to distinguish them from the coefficients of the desired multipath field Q_j . Therefore, also the effect of signal reflections is contained in the Z_j , which replace the probe coefficients P_j in (8) so that we get

$$\begin{bmatrix} Z_1^1 & Z_1^2 & \dots & Z_1^P \\ Z_2^1 & Z_2^2 & \dots & Z_2^P \\ \vdots & \vdots & \ddots & \vdots \\ Z_j^1 & Z_j^2 & \dots & Z_j^P \end{bmatrix} \begin{bmatrix} v_1 \\ v_2 \\ \vdots \\ v_p \end{bmatrix} = \begin{bmatrix} Q_1 \\ \vdots \\ Q_j \end{bmatrix}, \quad (10)$$

i.e., $\mathbf{Z}\mathbf{v} = \mathbf{q}$. The required probe excitations are then again solved by matrix inversion

$$\mathbf{v} = \mathbf{Z}^\dagger \mathbf{q} = (\mathbf{Z}^H \mathbf{Z})^{-1} \mathbf{Z}^H \mathbf{q}.$$

This technique can be applied even in environments, which have a high reflectivity level. It should be noted, though, that multiple reflections between the antenna under test (AUT) or the TZF probe and the surroundings are not accounted for, and will produce some errors if their level is high.

III. SIMULATIONS

In this section, we investigate the aforementioned synthesis techniques through simulations. The effects of the measurement noise and the truncation of the spherical-mode series are studied. The simulations are based on real propagation data, obtained from measurements in the Helsinki city center. These measurements are described in Section A. Section B then presents the simulation procedure.

A. Propagation Environment

The measurements of the propagation environment were conducted using a 5.3 GHz channel sounder [17] in the center of Helsinki, where the average building height is 5-8 storeys. The transmitter was elevated to approximately 10 m above the street, still being clearly below rooftop level, and the receiver was moved along the streets at 1.6 m above the street. The measurement environment includes line-of-sight and non-line-of-sight conditions and the measurement route is illustrated in Fig. 2.

The measurement system uses a pseudo-noise sequence with a chip frequency of 60 MHz and a code length of 255 samples. In the measurements, a dual-polarized planar 4x4 and a semi-spherical antenna structure were used in the transmitter (TX) and receiver (RX), respectively. The measurement system uses a switched-array measurement principle, where all the channel combinations between TX and RX elements are measured consecutively. The serial-form measurement data is measured in 8.8 ms, during which the channel is assumed to be time-invariant. In the post-processing this data is parallelized as a 32x32 MIMO channel matrix.

From each 32x32 MIMO channel matrix, measured 4-5

times per traveled wavelength, the direction-of-departure (DoD), direction-of-arrival (DoA), delay, and complex path weight parameters of the propagating waves were calculated using the SAGE algorithm [18].

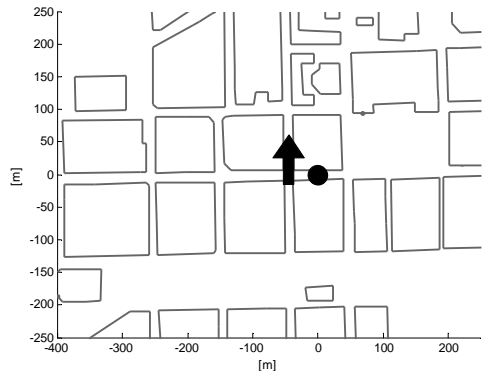


Fig. 2. Map of the measurement environment showing the transmitter (dot) and the moving receiver (arrow).

B. Simulation Procedure

In the simulation we study the signal received by a two-port (i.e. has two radiating elements) mobile terminal antenna model placed in the test zone. An antenna model with isotropic, vertically-polarized radiation pattern is used as the transmitter. We begin by converting the plane-wave propagation model of the previous section into a spherical-wave model, using the expansion in [10, A1.6]. This is done for each snapshot (moment of time) as the receiver moves along a predetermined route. The spherical wave model then contains the angles-of-arrival, complex amplitudes, and polarizations of all signal paths in the propagation model, given in the form of (7).

We need to first establish as a reference the true signal received by the AUT in the propagation environment in question. For this, we use a truncation number, which is very large considering the AUT size, and assume the truncation error to be negligible. We can, therefore, calculate as our reference case the signal w received by the AUT in the true propagation environment as [12, p.68]

$$w_{true} = \frac{1}{2} \sum_{j=1}^J R_j Q_j^{(1)}, \quad (10)$$

where $Q_j^{(1)}$ are the coefficients of the propagation model, R_j are the (known) receiving coefficients of the AUT, and $J = 240$, which corresponds to $N = 10$ according to (3). The radius of the AUT minimum sphere is approximately 0.35λ , for which (2) suggests $N = 3$.

The number of spherical modes that can be synthesized (and therefore, the truncation level) depends on the number of probes available for the synthesis. It is important to note that

the truncation error in the synthesis does not result from the non-existence of high-order modes in the test zone, but rather from erroneous high-order modes. The probe excitations will reproduce the low-order modes accurately, but in addition they will also produce high-order modes that cannot be controlled. The AUT will receive also these high-order modes and this results in the truncation error.

The simulation begins by the calculation of the probe coefficients (5) according to the probe configuration. The probes in the simulation are dipoles and they are arranged uniformly on a spherical surface surrounding the test zone. Half of the probes are θ -polarized and half φ -polarized. The matrix equation (8) is constructed and solved for the probe weights \mathbf{v} , using (9). We can then use the equations

$$Q_{j, \text{synth}}^{(1)} = \sum_{p=1}^P v_p P_j^p \quad (11)$$

and

$$w_{\text{synth}} = \frac{1}{2} \sum_{j=1}^J R_j Q_{j, \text{synth}}^{(1)} \quad (12)$$

to calculate the signal received by the AUT in the test zone. By comparison of w_{true} and w_{synth} with different values for P (the number of probes), we can investigate the effect of the truncation error.

We are also interested in the effect of measurement noise on the result. We will study this for the technique based on free-space assumption (Sec. II.B.1). Similar conclusions, however, hold for the technique based on TZF measurement, assuming the errors in the TZF measurement are not dominant. For this, we introduce noise to the probe weights in (11) so that $\mathbf{x} = \mathbf{v} + \mathbf{n}$, where \mathbf{n} is a (Gaussian) noise vector of the same size as \mathbf{v} . Then, the spherical mode coefficients of the synthesized test zone field produced by the noisy probe excitations \mathbf{x} , are calculated as

$$Q_{j, \text{synth}}^{(1)} = \sum_{p=1}^P x_p P_j^p. \quad (13)$$

Otherwise, the procedure is the same as above.

IV. RESULTS

The results of the simulations are presented for different probe configurations, i.e., the number of probes is varied according to Table I. Table I also shows the truncation number and the number of spherical modes that are synthesized with each probe configuration.

The normalized error vector amplitude ζ between w_{true} and w_{synth} is calculated as

$$\zeta = \frac{|w_{\text{true}} - w_{\text{synth}}|}{\max |w_{\text{true}}|} \quad (14)$$

The denominator in this equation is the global maximum of the received signal in the true propagation environment, considering all snapshots (the max-mean ratio of w_{true} is 6 dB). The error vector amplitude is calculated separately for each snapshot. The root-mean-square value of ζ is presented in Fig. 3 for both AUT ports as a function of the number of probes for different noise levels in the probe stimuli. The RMS noise vector magnitude is shown in dB relative to the maximum probe signal amplitude. The max-mean ratio of the probe stimuli rises with the number of probes, going from 17 dB (24 probes) to 28 dB (212 probes).

Table I. The number of probes and the corresponding number of synthesized spherical modes in the simulation.

Truncation number (N)	Number of modes (J)	Number of probes (P)
2	16	24
3	30	44
4	48	68
5	70	92
6	96	128
7	126	164
8	160	212

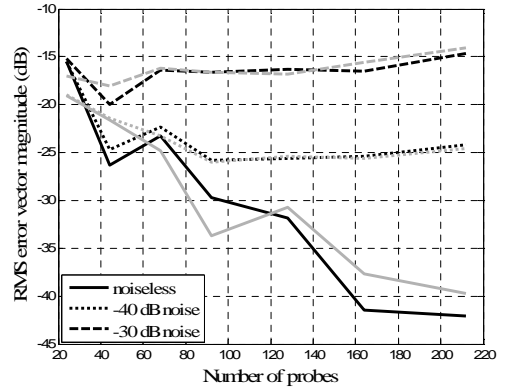


Fig. 3. The normalized RMS error vector magnitude in the signal received by the AUT in the synthesized multipath environment (gray = port 1, black = port 2).

It is clear from Fig. 3 that in the absence of measurement noise, the error vector magnitude decreases as the number of probes increases, as expected. The curves are not, however, entirely smooth. For example, at some points, the effect of high-order modes that cannot be reproduced with a given number of probes tends to cancel out. This effect is a combination of the AUT and the propagation environment

characteristics. Nevertheless, overall the accuracy of the synthesis increases with the number of probes used.

The situation is different, when we introduce noise to our probe stimuli. Fig. 3 shows that in this case, the addition of probes does not improve the result after a certain point. For example, with -30 dB noise level, similar results are obtained with 20 and 200 probes. Of course, these considerations are dependent on the electrical size of the AUT, which is in our case slightly less than one wavelength. But once the measurement-noise level and the size of the AUTs to be tested are known, the number of probes can be selected so that the desired accuracy can be achieved.

Fig. 4 depicts the signal levels received by the two ports of the AUT as a function of snapshot, i.e., as the AUT moves along the measurement route. The noise level in the probe stimuli is -40 dB and the number of probes used for the synthesis is 44 (22 for each polarization), with truncation number $N = 3$. This truncation number corresponds to criterion (2) and, as can be seen from Fig. 4, produces a good result. The relative amplitudes of the signals received by the two ports of the AUT vary significantly, but are very similar in the synthesized and true environments.

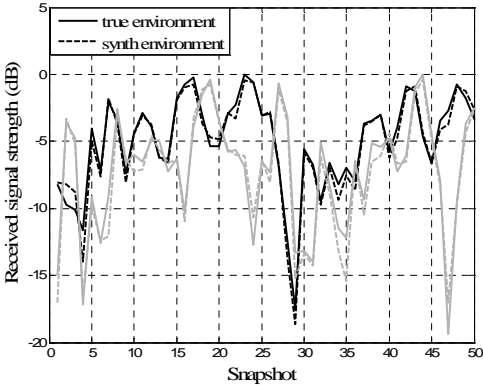


Fig. 4. The signal levels received by the two ports of the AUT in the true environment compared to the synthesized environment with 30 modes (gray = port 1, black = port 2).

A typical parameter of interest in multi-antenna systems is the channel capacity. In the general case, the capacity C can be calculated as [19]

$$C = \log_2 \left(\det \left(\mathbf{I}_{N_r} + \frac{\rho}{N_t} \mathbf{H} \mathbf{H}^H \right) \right), \quad (15)$$

where \mathbf{I}_{N_r} is the identity matrix, ρ is the signal-to-noise ratio, \mathbf{H} is the channel matrix, and N_t and N_r are the number of transmit and receive antennas, respectively. In these simulations, $N_t = 1$ and $N_r = 2$. Thus, we are dealing with a single-input multiple-output (SIMO) radio channel. We can calculate the channel matrix \mathbf{H} from the AUT received-signal

values (Fig. 4). Furthermore, for the capacity calculation we use $\rho = 10$ dB and the Frobenius norm normalization

$$\langle \|\mathbf{H}\|_F^2 \rangle = N_r N_t, \quad (16)$$

where $\langle \cdot \rangle$ stands for average over time.

The cumulative distribution function of the capacity is presented in Fig. 5 for the true environment and for some synthesized environments with different truncation numbers (and -40 dB relative noise level). It can be seen that the calculated capacity is very close to the true with $N = 3$ (44 probes). This is not surprising since Fig. 4 shows that the signal levels in the synthesized environment are very close to the true environment. However, $N = 2$ (24 probes) produces equally good results for the capacity. Only with $N = 1$ (6 modes and 8 probes) a noticeable difference occurs. This is more evident from Fig. 6, where the error in the capacity is plotted against the cumulative probability. With $N = 3$ and $N = 2$ the error remains approximately within ± 0.1 bit/s/Hz and with $N = 1$ within ± 0.3 bit/s/Hz. Somewhat larger errors are seen at very low and high probability levels, where the number of samples is small. The distributions were calculated from 1000 samples each.

This analysis shows that, even though the errors in the received signal increase with very small truncation numbers, good results can still be obtained for statistical parameters. In other words, criterion (2) need not necessarily be satisfied in the measurement of statistical parameters. This is important because statistical behaviour of parameters like capacity is a relevant figure of merit in the OTA testing of MIMO systems.

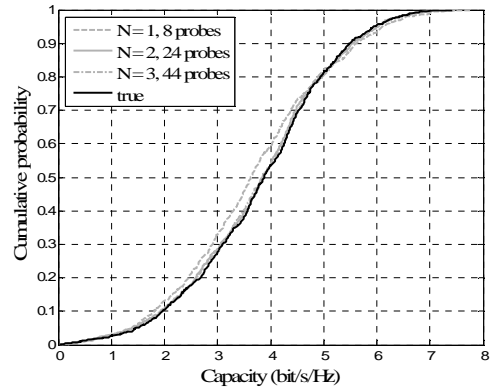


Fig. 5. Capacity of the simulated SIMO communications channel in the true environment and in the synthesized environment with different numbers of probes.

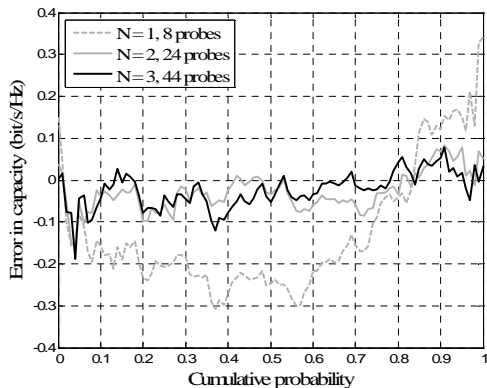


Fig. 6. Error in capacity in the cumulative distribution function for different numbers of probes in the synthesis.

V. CONSIDERATIONS ON PRACTICAL IMPLEMENTATION

There are many things to be considered in a practical implementation of a system that can synthesize radio channel environments in a manner presented in this paper.

First, there is the probe configuration, which includes the number, placement and type of the probes. The type of the probes is not restricted, nor do they need to be identical, so it is possible to use inexpensive antennas in the system. However, if the system is designed to be operated over a wide frequency band, the probes should be wideband as well. The use of directive probes reduces reflections from the environment and may thus improve the performance of the system.

The AUT size and the desired measurement accuracy determine the required truncation number and thus also the number of probes. According to the simulations, criterion (2) seems to produce good results at least for small AUTs.

Even though in typical propagation scenarios signals do not usually arrive from all directions, there are advantages to placing the probes so that they surround the test zone uniformly. In this way, the system is very versatile and it becomes, for example, possible to “code” the change of the AUT orientation to the synthesis so that instead of tilting the mobile phone the whole propagation environment can be tilted in the test zone. This might represent the effect of a user changing the orientation of the mobile phone.

Second, we need to have hardware to feed the probes in an appropriate manner. Radio channel emulators are able to produce the required channel effects for multiple parallel channels. However, in order to synthesize these channels in the spatial domain, we need to be able to distribute the signals to the probes. This requires a large signal distribution network with amplitude and phase control for each path. As the number of probes increases, such a network becomes more and more complicated. This is why, at present, the implementation of this kind of systems for large AUTs may not be feasible.

Third, the system requires control software. Due to the

computational burden, it may be necessary to compute the coefficients and required control parameters offline before the synthesis is performed. This is not a problem, though, as the parameters related to each propagation environment can be stored in a file and run from there.

VI. CONCLUSION

We have presented a way to synthesize arbitrary multipath radio-channel environments in laboratory conditions. The error introduced in the synthesis due to a limited number of probes is bounded and can be, in theory, made as small as desired by selecting an appropriate number of probes [14]. The results indicate that for a typical urban environment considered in this paper and a mobile terminal antenna structure of typical size, the channel capacity can be measured at ± 0.1 bit/s/Hz uncertainty with $N = 2$ and at ± 0.3 bit/s/Hz uncertainty with $N = 1$.

Although propagation models are typically based on far-field assumptions, the presented method is not limited to far-field models, but can be applied to synthesize arbitrary electromagnetic environments, including near-field effects. This property arises from the spherical-wave theory, on which the method is based.

Obvious applications are found in the testing of mobile terminals, but also any other task requiring a certain electromagnetic field distribution in a limited volume of space (e.g., electromagnetic compatibility testing) might make use of this method.

REFERENCES

- [1] J. Krogerus, P. Mäkiyryö, and P. Vainikainen, “Towards an applicable OTA test method for multi-antenna terminals,” COST2100 TD(08) 671, Lille, France, October 2008.
- [2] T. A. Laitinen *et al.*, “From the radiation pattern measurements towards true performance evaluation of mobile terminal antennas,” in *Proc. 2nd Eur. Conf. Antennas and Propagation (EuCAP2007)*, CD-ROM, November 2007.
- [3] P. Suvikunnas, J. Villanen, K. Sulonen, C. Icheln, J. Ollikainen, and P. Vainikainen, “Evaluation of the performance of multiantenna terminals using a new approach,” *IEEE Trans. Instrum. Meas.*, vol. 55, no. 5, pp. 1804-1813, October 2006.
- [4] P. S. Kildal, “Overview of 6 years R&D on characterizing wireless devices in Rayleigh fading using reverberation chamber,” in *Proc. International Workshop on Antenna Technology: Small and Smart Antennas, Metamaterials and Applications (IWAT'07)*, pp. 162-165, March 2007.
- [5] H. Iwai, A. Yamamoto, T. Sakata, K. Ogawa, K. Sakaguchi, and K. Araki, “Spatial fading emulator for handset antennas,” in *Proc. Antennas and Propagation Society International Symposium*, vol. 1A, pp.218-221, July 3-8, 2005.
- [6] A. Yamamoto, T. Sakata, H. Iwai, K. Ogawa, J. Takada, K. Sakaguchi, and K. Araki, “BER measurements on a handset adaptive antenna array in the presence of cochannel interference generated using a spatial fading emulator,” in *Proc. Antennas and Propagation Society International Symposium*, vol. 4A, pp.26-29, July 3-8, 2005.
- [7] P. Kyösti, J. Kolu, J. Nuutinen, M. Falck, and P. Mäkiyryö, “OTA testing for multiantenna terminals,” COST2100 TD(08) 670, Lille, France, October 2008.
- [8] M. A. Poletti, “Three-dimensional surround sound systems based on spherical harmonics,” *J. Audio Eng. Soc.*, vol. 53, no. 11, pp. 1004-1025, November 2005.
- [9] D. B. Ward, T. D. Abhayapala, “Reproduction of a plane-wave sound field using an array of loudspeakers,” *IEEE Trans. Speech Audio Process.*, vol. 9, no. 6, pp. 697-707, September 2001.

- [10] EB Radio Channel Emulator product description. Available: http://www.elektrobit.com/what_we_deliver/wireless_communications_tools/products/eb_propsim_f8
- [11] T. Laitinen, "Advanced spherical antenna measurements," D.Sc. dissertation, Radio Laboratory, Helsinki Univ. Tech., Helsinki, Finland, 2005.
- [12] J.E. Hansen, Ed., *Spherical Near-Field Antenna Measurements*, London, UK: Peter Peregrinus Ltd., 1988.
- [13] H. M. Jones, R. A. Kennedy, and T. D. Abhayapala, "On dimensionality of multipath fields: Spatial extent and richness," in *Proc. IEEE Int. Conf. Acoust., Speech Signal Process. (ICASSP)*, Orlando, FL, May 2002, pp. 2837-2840.
- [14] R. A. Kennedy, P. Sadeghi, T. D. Abhayapala, and H. M. Jones, "Intrinsic limits of dimensionality and richness in random multipath fields," *IEEE Trans. Sign. Process.*, vol. 55, no. 6, pp. 2542-2556, June 2007.
- [15] G. H. Golub, and C. F. Van Loan, *Matrix computations*, 3rd ed., Baltimore, MD: The Johns Hopkins Univ. Press, 1996.
- [16] J. T. Toivanen, T. Laitinen, P. Vainikainen, "Modified test zone field compensation for small-antenna measurements," *IEEE Trans. Ant. Propag.*, to be published.
- [17] V.-M. Kolmonen, J. Kivinen, L. Vuokko, and P. Vainikainen, "5.3 GHz MIMO radio channel sounder," *IEEE Trans. Instrum. Meas.*, vol. 55, no. 4, pp. 1263-1269, Aug. 2006.
- [18] B. Fleury, P. Jourdan, and A. Stucki, "High-resolution channel parameter estimation for MIMO applications using the SAGE algorithm," in *Proc. International Zurich Seminar on Networking Broadband Communications*, pp. 30-1 - 30-9, 2002.
- [19] G. J. Foschini, "Layered space-time architecture for wireless communication in a fading environment when using multi-element antennas," *Bell Labs Tech J.*, pp. 41-59, Autumn, 1996.